[Article] doi: 10.3866/PKU.WHXB201206271 www.whxb.pku.edu.cn

介孔氧化铝负载Ni-Co氧化物催化剂上丙烷氧化脱氢制丙烯

孙毅飞 李广超 潘心頓 黄传敬* 翁维正 万惠霖*
(固体表面物理化学国家重点实验室, 醇醚酯清洁生产国家工程实验室, 厦门大学化学化工学院化学系, 福建 厦门 361005)

摘要: 以非离子型三嵌段共聚物作为模板剂, 异丙醇铝为氧化铝的前驱物, 采用一锅法合成了一系列介孔氧化铝负载镍氧化物、钴氧化物以及镍-钴双金属氧化物催化剂, 并以介孔氧化铝为载体, 采用浸渍法制备了负载Ni-Co氧化物催化剂. 采用N_2吸附-脱附、高分辨透射电镜(HRTEM)、X射线粉末衍射(XRD)、H_2程序升温还原(H_2-TPR)以及激光拉曼光谱(LRS)等技术对催化剂的结构与性质进行表征, 并考察了催化剂的丙烷氧化脱氢反应性能. 结果表明: 一锅法制备的各催化剂均有大的比表面积和规整的孔道结构, 且负载的金属氧化物高度分散; 而浸渍法制备的催化剂, 其载体的介孔结构被破坏并有Co_3O_4晶相生成. 在考察的催化剂中, 一锅法合成的介孔氧化铝负载Ni-Co氧化物催化剂表现出最佳的丙烷氧化脱氢性能. 在450 °C、C_3H_8:O_2:N_2的摩尔比为1:1:4和空速(GHSV)为10000 mL·g^{-1}·h^{-1}条件下, 该催化剂上丙烯产率为10.3%, 远高于浸渍法制备的催化剂上所获得的丙烯产率(2.4%). 关联催化剂表征和反应结果, 讨论了催化剂结构与性能之间的关系.

关键词: 丙烷; 丙烯; 氧化脱氢; Ni-Co氧化物催化剂; 介孔氧化铝; 一锅法
中图分类号: O643

Oxidative Dehydrogenation of Propane to Propylene over Mesoporous Alumina Supported Ni-Co Oxide Catalysts

SUN Yi-Fei LI Guang-Chao PAN Xin-Di HUANG Chuan-Jing*
WENG Wei-Zheng WAN Hui-Lin*
(*State Key Laboratory of Physical Chemistry of Solid Surfaces, National Engineering Laboratory for Green Chemical Productions of Alcohols, Ethers and Esters, Department of Chemistry, College of Chemistry and Chemical Engineering, Xiamen University, Xiamen 361005, Fujian Province, P. R. China*)

Abstract: A series of mesoporous alumina supported nickel oxide, cobalt oxide, and bimetallic nickel-cobalt oxide catalysts were synthesized by a one-pot method, using nonionic triblock copolymer as a template and aluminum isopropoxide as the source of aluminum. For comparison, an additional supported Ni-Co oxide catalyst was prepared by impregnation, using mesoporous alumina as the support. The catalysts were tested for the oxidative dehydrogenation of propane, and their structure and properties were characterized by N_2 adsorption-desorption, high-resolution transmission electron microscopy (HRTEM), powder X-ray diffraction (XRD), temperature-programmed H_2 reduction (H_2-TPR), and laser Raman spectroscopy (LRS). All samples synthesized by the one-pot method had large surface area, highly ordered mesoporous structure, and highly dispersed supported oxide species. However, in the sample prepared by impregnation, the mesostructure of the carrier was destroyed with the formation of Co_3O_4 phase. Among the catalysts studied, the mesoporous alumina supported Ni-Co oxide catalyst from one-pot synthesis

Received: April 18, 2012; Revised: June 26, 2012; Published on Web: June 27, 2012.
*Corresponding authors. HUANG Chuan-Jing, Email: huangcj@xmu.edu.cn; Tel: +86-592-2188087. WAN Hui-Lin, Email: hlwan@xmu.edu.cn.
The project was supported by the National Key Basic Research Program of China (973) (2010CB732303), National Natural Science Foundation of China (21173173, 21073148, 21033006), Program for Innovative Research Team of the Ministry of Education of China (IRT1036), National Foundation for Fostering Talents of Basic Science, China (J1030415), and Key Scientific Project of Fujian Province, China (2009HZ0002-1).
国家重点基础研究发展规划项目(973) (2010CB732303), 国家自然科学基金(21173173, 21073148, 21033006), 教育部创新团队项目(IRT1036), 国家基础科学人才培养基金(J1030415)和福建省重大科技专项(2009HZ0002-1)资助

showed the best catalytic performance for propane oxidation to propylene. On this catalyst a 10.3% propylene yield was obtained at 450 °C, C_3H_8:O_2:N_2 molar ratio of 1:1:4, and gas hourly space velocity (GHSV) of 10000 mL·h^{-1}·g^{-1}. This result was much higher than the yield of 2.4% obtained from the catalyst prepared by impregnation. Combining the results of characterization and catalytic reaction, the relationship between structure and performance of the catalysts was discussed. The large difference observed in catalytic performance between catalysts prepared by one-pot and impregnation methods was attributed to their different structures, including textural structure, and dispersion of the supported metal oxide species.

Key Words: Propane; Propylene; Oxidative dehydrogenation; Ni-Co oxide catalyst; Mesoporous alumina; One-pot method

1 Introduction

Propylene is an important feedstock for the petrochemical industry as it is used for the synthesis of various chemical intermediates and major processes such as polypropylene synthesis. At the present time, propylene is produced mainly through catalytic cracking, stream cracking, and catalytic dehydrogenation. However, these processes require operation at relatively high temperatures and thus high-energy costs. Hence, the oxidative dehydrogenation of propane (ODHP), an alternative to the traditional processes, has attracted increasing attention due to its higher efficiency of using light alkane resource with minimum energy consumption. A large variety of unsupported and supported oxide catalysts have been reported to be active for the ODHP reaction. Most of those catalysts described in the literature are based on vanadium or molybdenum.[1−6] Recently, it was reported that mesostructured NiO[7] and nanosized Co_3O_4[8] were also effective in the ODHP reaction, especially at low temperatures. These unsupported oxide catalysts, however, are less stable because they could be sintered and/or reduced easily at higher temperatures. Thus, the supported nickel and cobalt oxide catalysts with a suitable support that can disperse and stabilize the active phase are highly desired.

With the development of SBA-15,[9] the mesoporous materials began to attract much attention because of their highly uniform channels, large surface area, narrow pore-size distribution, and tunable pore sizes. All these advantages are beneficial for catalytic reactions. Among various mesoporous materials, the mesoporous alumina should be placed high priority because of its tunable acid-base character, excellent mechanical strength, and wide application of commodity alumina. The first successful synthesis of ordered mesoporous alumina (OMA) using block copolymer surfactant as template was reported by Niesz *et al*.,[10] but this procedure required a strict control of experimental conditions. A significant improvement in the preparation of OMA has been achieved by Yuan *et al*.,[11] who reported a reliable and reproducible preparation method for OMA, based on self-assembly of the Pluronic P123 ($EO_{20}PO_{70}EO_{20}$) (EO: ethylene oxide, PO: propylene oxide) triblock copolymer and alumina precursors in ethanolic solution in the presence of additives such as citric or nitric acid. This strategy was extended by Stacy *et al*.[12] to the one-spot synthesis of metal oxide supported ordered mesoporous alumina. Based on these results, ordered mesoporous Ni-Mg-Al oxides were also prepared and tested for steam reforming of methane.[13] However, very limited studies have been made on the mesoporous alumina supported nickel or cobalt oxide catalysts for the ODHP reaction. Especially, no any studies have been made for the preparation and catalytic application of ordered mesoporous Ni-Co-Al oxide materials.

In this work, we report the results of a study on the preparation, characterization, and activity of OMA supported nickel-cobalt oxide catalysts for the ODHP reaction. For comparison, OMA supported nickel or cobalt oxide catalysts were also investigated.

2 Experimental

2.1 Catalyst preparation

A series of mesoporous alumina (MA) supported nickel and/or cobalt oxide catalysts were prepared by one-pot synthesis using a modified procedure based on previous report.[12] Typically, 4.5 g of $(EO)_{20}(PO)_{70}(EO)_{20}$ triblock copolymer (P123) (Aldrich, AR, *M*=5800) was dissolved in 100 mL anhydrous ethanol (AR) at room temperature, after the dissolution of P123, 7.5 mL 65% (*w*) HNO_3 (AR) and 10.2 g aluminum isopropoxide (CP) were added into the above solution with vigorous stirring for about 5 h with the cover of polyethylene (PE) films. Then, quantitative nickel nitrate (AR) and cobalt nitrate (AR) were added into the solution with vigorous stirring for 5 h. The solvent was evaporated at 60 °C for 48 h in the oven. The resulting samples were calcined at 400 °C for 4 h with a heating rate of 1 °C·min^{-1} and calcined at 600 °C for 1 h with a heating rate of 10 °C·min^{-1}. The synthesized catalysts were denoted as *x*Ni*y*Co-MA, where *x* and *y* refer to mass fractions of Ni and Co in the catalyst, respectively.

For comparison, MA-supported nickel and cobalt oxide catalysts were also prepared by impregnation method and denoted as *x*Ni*x*Co/MA. Briefly, the support MA, which was synthesized according to the procedure reported by Yuan and coworkers,[11] was impregnated with an aqueous solution of $Co(NO_3)_2$ and $Ni(NO_3)_2$, followed by drying and calcining at 600 °C for 4 h.

2.2 Catalyst characterization

XRD patterns were recorded on a Panalytical X′pert PRO

power diffractometer with Cu K_α radiation. N_2 adsorption-desorption isotherms were recorded at 77 K on an automated micromeritics Tri-Star 3000 apparatus. Surface areas were calculated using the multipoint BET equation. Pore size distributions were calculated by the BJH method using the desorption branch of the isotherm. The transmission electron microscopy (TEM) images were obtained from a FEI Tecnai-F30 FEG instrument with an acceleration voltage of 300 kV. H_2-TPR experiments were performed on a flow apparatus using a 5% H_2/Ar mixture flowing at 20 mL·min^{-1}. The heating rate was 10 °C·min^{-1}. Hydrogen consumption was monitored by a thermal conductivity detector (TCD) after removing the water formed. Laser Raman spectroscopy (LRS) was measured using Renishaw UV-Vis Raman 1000 System equipped with a charge coupled device (CCD) detector and a Leica DMLM microscope. The line at 514.5 nm of an Ar^+ laser was used for excitation.

2.3 Catalytic reaction

The oxidative dehydrogenation of propane was carried out in a fixed bed flow reactor under atmospheric pressure. For each testing, 0.1 g of catalyst was loaded in a quartz tubular reactor (i.d. 5 mm), and the feed gas of C_3H_8:O_2:N_2 (n(C_3H_8):n(O_2):n(N_2)=1:1:4) was passed through the reactor at a GHSV of 10000 mL·g^{-1}·h^{-1}. The products were analyzed by an online gas chromatograph equipped with a Porapak Q and a 5A molecular sieve column.

3 Results and discussion

3.1 Characterization of catalysts

The results of N_2 adsorption-desorption measurements are shown in Fig.1 and Table 1. As shown in Fig.1a, all the samples prepared by direct synthesis (MA, 10Ni-MA, 10Co-MA, and 10Ni10Co-MA) present typical type IV isotherms with H1 shaped hysteresis loops, suggesting their uniform cylindrical pores. From the BJH pore size distributions shown in Fig.1b, it can be seen that these samples possess uniform mesoporous structure. This observation is significant, since it demonstrates that the strategy for preparation of OMA reported by Yuan *et al.*[11] can be extended to the one-pot synthesis of alumina-supported mixed oxide catalysts with an ordered mesoporous structure. On the other hand, 10Ni10Co/MA, the sample prepared by impregnation method shows the small adsorption quantity and broad capillary condensation step, indicating the collapse of ordered meso-structure. As shown in Table 1, all the catalysts investigated show an expected decrease in BET surface area (S_{BET}), due to the introduction of Ni and/or Co oxide species into alumina. However, the surface area of 10Ni10Co/MA prepared by impregnation is significantly lower than that of 10Ni10Co-MA by direct synthesis, although both samples have the same Ni and Co contents. Moreover, the sample by impregnation possesses much smaller pore volume (V_{sp}) and pore size, indicating the destruction of mesoporous structure probably due to the impregnation procedure and/or the aggregation of the supported oxide species.

Table 1 Surface areas and pore structures of various samples

Catalyst	S_{BET}/(m^2·g^{-1})	V_{sp}/(cm^3·g^{-1})	Pore size/nm
MA	281	0.84	8.3
10Ni-MA	249	0.67	8.9
10Co-MA	241	0.83	8.7
10Ni10Co-MA	209	0.67	10.8
10Ni10Co/MA	189	0.31	4.5

The TEM images shown in Fig.2 demonstrate the structures of the catalysts more directly and visually. It is quite manifest that the 10Ni10Co-MA catalyst has the uniform and hexagonally ordered mesopores with *p*6*mm* symmetry and honeycomb structure. What is more, no aggregation of nickel and/or cobalt oxide particles could be observed in 10Ni10Co-MA, which proves that the active species on the catalyst are high-dispersed. Conversely, the image of 10Ni10Co/MA demonstrates a worm-like structure which indicates the destruction of mesopority.

The XRD patterns of various catalysts are shown in Fig.3. All the catalysts synthesized by one-pot method present XRD patterns without any diffraction peaks, indicating that the oxide species on these samples are high-dispersed. On the other hand, 10Ni10Co/MA catalyst exhibits a quite different XRD pattern, where five diffraction peaks ascribed to Co_3O_4 or $CoAl_2O_4$[14] are clearly observed at 31.3°, 36.8°, 45.6°, 59.4°, and 65.4°, respectively. This indicates that the cobalt oxide species are less dispersed on the catalyst prepared by impregnation method.

The H_2-TPR results of various catalysts are shown in Fig.4. For 10Ni-MA catalyst, only one reduction peak could be identi-

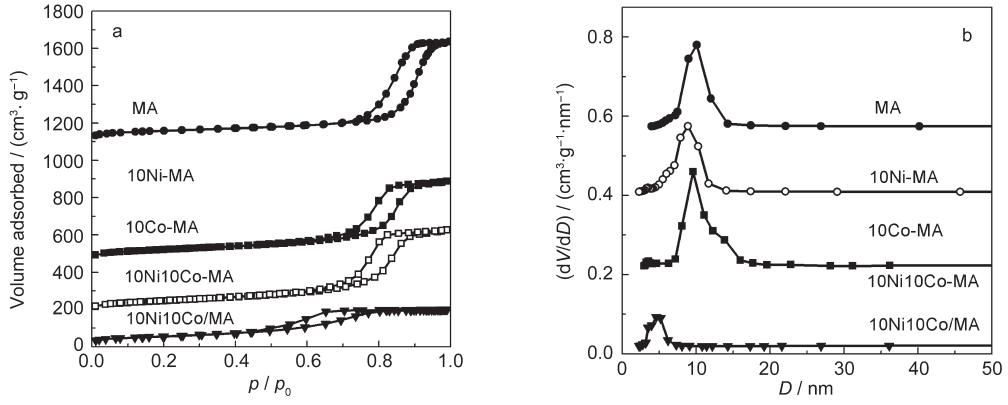

Fig.1 N_2 adsorption-desorption isotherms (a) and BJH pore diameter (D) distributions (b) of various catalysts

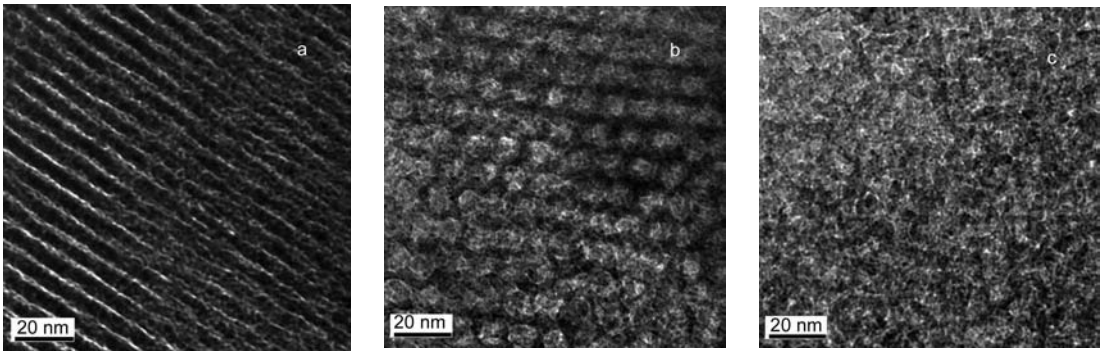

Fig.2 TEM images of 10Ni10Co-MA (a, b) and 10Ni10Co/MA (c) catalysts

electron beam perendicular (a) and parallel (b) to the main axis of the pores

fied at approximately 570 °C, which has been attributed to the reduction of nickel-aluminum solid solution by Kobayashi and co-workers.[15] On 10Co-MA, one major reduction peak appears at about 800 °C, which can be ascribed to the high-dispersed Co species that interact strongly with alumina.[16] 10Ni10Co-MA catalyst shows a TPR profile where two major peaks are centered at 570 and 700 °C, in a manner resembling a combination of profiles of the two supported mono-oxide catalysts, which indicates the presence of both the nickel-aluminum solid solution and the high-dispersed Co species in this sample. The reduction peak of Co species shifts to lower temperature, as compared to that of 10Co-MA catalyst. This could be attributed to the decrease of interaction of Co species with alumina, or ascribed to the hydrogen spillover generated by Ni species that promotes the reduction of cobalt oxides. Furthermore, a very weak at around 260 °C is also observed for both 10Ni10Co-MA and 10Co-MA catalysts. This peak is due to the reduction of a trace amount of free Co_3O_4 which is below the XRD detection limit. 10Ni10Co/MA catalyst presents a quite different TPR profile, as compared to that of 10Ni10Co-MA catalyst. On 10Ni10Co/MA two large low-temperature peaks are observed at 260 and 320 °C. Since the intensity ratio of the second peak to the first peak was close to 3:1, the two peaks could be attributed to the two-sep reduction of Co_3O_4 ($Co_3O_4 \rightarrow CoO \rightarrow Co$).[17] This indicates that a large amount of Co species aggregate into Co_3O_4, which is evidenced by the decrease of the reduction peak of high-dispersed Co species at about 750 °C. These results are also in accordance with XRD results. For this catalyst, the TPR peak due to the dispersed Co species shifts to a higher temperature (~750 °C) than that of 10Ni10Co-MA, revealing a weaker interaction between nickel and cobalt species in the impregnated sample.

The XRD and TPR results were further confirmed by the Raman spectra of the catalysts. As shown in Fig.5, no Raman peaks could be detected for all the catalysts prepared by one-pot synthesis, indicating that their supported oxide species are highly dispersed. For 10Ni10Co/MA sample, however, several distinct peaks due to Co_3O_4[18] are observed at 192, 477, 518, 614, and 684 cm^{-1}. This result implies that the surface of the catalyst is covered with a Co_3O_4 phase.

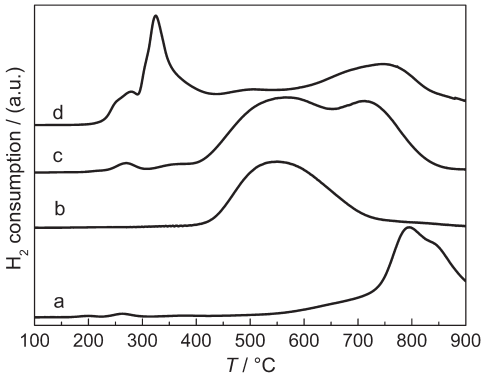

Fig.4 H_2-TPR patterns of 10Co-MA (a), 10Ni-MA (b), 10Ni10Co-MA (c), and 10Ni10Co/MA (d) catalysts

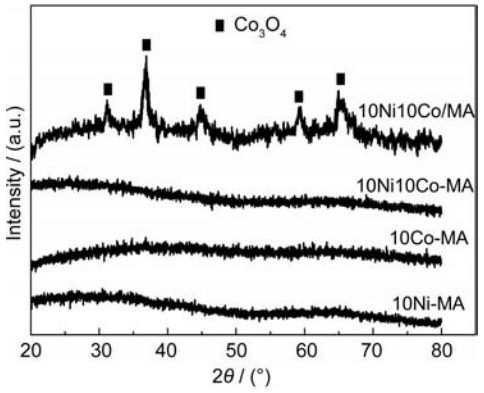

Fig.3 XRD patterns of various catalysts

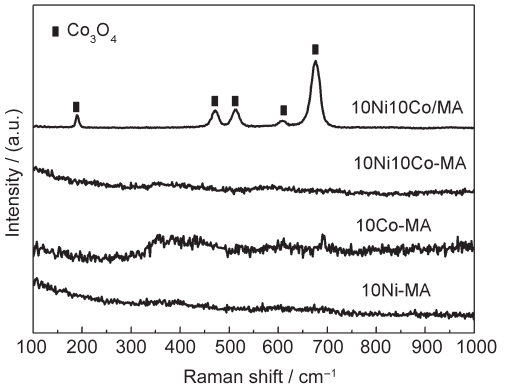

Fig.5 Raman spectra of various catalysts

3.2 Catalytic performance for the ODHP reaction

The catalytic performances of the various catalysts for ODHP reaction at 450 °C are compared in Table 2. It can be found that the catalysts prepared by one-pot synthesis show different catalytic performance depending on composition. 10Ni-MA catalyst shows a poor activity for propane conversion, although the selectivity to propylene is as high as 62.6%. 10Co-MA catalyst exhibits a high propane conversion, but its propylene selectivity is quite low. Compared with the two supported mono-metal oxide catalysts, the supported binary oxide systems (5Ni5Co-MA and 10Ni10Co-MA) show much better catalytic performance for ODHP to propylene, in terms of higher propane conversion and higher propylene yield. These results demonstrate the synergetic effect between Ni and Co oxide species, which can largely improve the catalytic performance of the catalyst.

For the alumina supported Ni-Co oxide catalyst, the effect of preparation method is also shown in Table 1. It is interesting to note that the catalytic behavior of the catalyst is significantly affected by the preparation method. 10Ni10Co/MA, the catalyst prepared by impregnation shows a very low selectivity to propylene, although its propane conversion is very high. Over this sample, propylene yield is only 2.4%, which is much lower than that of the sample prepared by one-pot synthesis.

Fig.6 shows the catalytic performance of 10Ni10Co-MA and 10Ni10Co/MA catalysts for ODHP as a function of temperature. Compared with the catalyst prepared by impregnation, the catalyst synthesized by one-pot method shows the outstanding selectivity towards propylene with a higher propylene yield at each reaction temperature. Although 10Co10NiO/MA exhibits much higher propane conversion in all the range of temperature examined, the deep oxidation reaction is so severe that more than 90% of the products are CO and CO_2, which leads to its very low propylene yield.

The stability of a catalyst is very important in the view of potential industrial application. So the stability of 10Ni10Co-MA catalyst was investigated by recording the catalytic performance for 12 h on-line at settled reaction conditions (T=450 °C, GHSV=10000 mL·g^{-1}·h^{-1}, $n(C_3H_8):n(O_2):n(N_2)$=1:1:4). The result of the stability test is presented in Fig.7. It can be seen that propane conversion, propylene selectivity, and propylene yield maintain their initial values without significant variation during the 12 h catalytic reaction, indicating the high stability of 10Ni10Co-MA catalyst.

Table 2 Catalytic performances of various catalysts for ODHP reaction

Catalyst	C_3H_8 conversion/%	Selectivity/%		C_3H_6 yield/%
		C_3H_6	CO_x	
10Ni-MA	12.3	62.6	37.4	7.6
10Co-MA	22.3	28.6	71.4	6.4
5Ni5Co-MA	26.4	38.4	61.6	10.1
10Ni10Co-MA	25.0	41.4	58.6	10.3
10Ni10Co/MA	41.5	6.0	94.0	2.4

reaction conditions: GHSV=10000 mL·g^{-1}·h^{-1}; $n(C_3H_8):n(O_2):n(N_2)$=1:1:4; T=450 °C

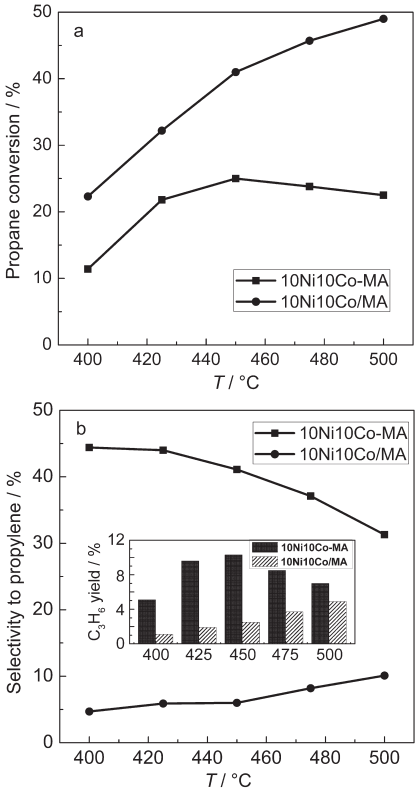

Fig.6 Propane conversion (a), propylene selectivity and yield (b) on 10Ni10Co-MA and 10Ni10Co/MA catalysts at different temperatures

reaction conditions: GHSV=10000 mL·g^{-1}·h^{-1}; $n(C_3H_8):n(O_2):n(N_2)$=1:1:4

The significant difference in catalytic performance between 10Ni10Co-MA and 10Ni10Co/MA catalysts could be attributed to several structural factors. First of all, as shown in N_2 adsorption-desorption and TEM, the catalysts prepared by one-pot and impregnation methods show quite different textural structures. 10Ni10Co-MA, the sample by one-pot synthesis has a highly ordered mesoporous structure, with large surface area and high porosity. This structure can allow efficient molecular transport by diffusion in the channels during the ODHP reac-

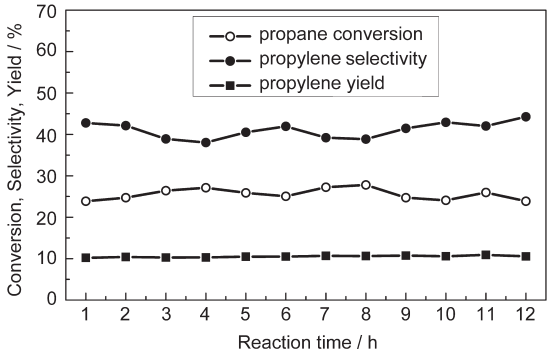

Fig.7 Alteration of propane conversion, propylene selectivity and propylene yield as a function of time on stream over 10Ni10Co-MA catalyst

reaction conditions: GHSV=10000 mL·g^{-1}·h^{-1}; $n(C_3H_8):n(O_2):n(N_2)$=1:1:4; T=450 °C

tion, thus suppressing the consecutive oxidation of propylene to CO and CO_2 and increasing the selective conversion of propane to propylene. Furthermore, the structures of the supported oxides which serve as catalytically active phase for the ODHP reaction are also largely different for the catalysts prepared by different methods. As demonstrated by the results of XRD, TPR, and Raman spectra, both nickel and cobalt oxide species in 10Ni10Co-MA catalyst are highly dispersed, whereas large crystal Co_3O_4 is found on 10Ni10Co/MA catalyst. This observation is significant, since for the supported oxide catalysts including V-, Ni-, and Co-based catalysts,[3,19–24] the high-dispersed oxide species have been found to be active and selective for the dehydrogenation of light alkanes. Recently, based on the results obtained over CoMgAlO mixed oxide, it has been proposed that the well-dispersed cobalt species with tetrahedral coordination played a main role in the ODHP reaction while the spinel Co_3O_4 phase was responsible for CO_x formation.[25] This supposition can explain the different catalytic performances of 10Ni10Co-MA and 10Ni10Co/MA catalysts observed in this work.

4 Conclusions

In this work, a series of alumina supported nickel, cobalt, and nickel-cobalt oxide catalysts have been synthesized through a sol-gel route in one pot and tested for the oxidative dehydrogenation of propane to propylene. The supported Ni-Co oxide catalyst was also prepared by impregnation method, using mesoporous alumina as a support. All the samples prepared by one-pot synthesis showed an ordered mesoporous structure and high-dispersed metal oxide species, in contrast with the impregnated sample where the mesostructure was destroyed and crystalline Co_3O_4 could be observed. A synergetic effect between Ni and Co oxide species was observed for the supported Ni-Co oxide catalyst synthesized by one-pot method. Among the catalysts investigated, this catalyst showed the best catalytic performance for propane oxidation to propylene. On this catalyst, a propylene yield of 10.3% was obtained at 450 °C. The yield is much higher than that obtained over the catalyst prepared by impregnation (2.4%). This significant difference in catalytic performance between the catalysts prepared by one-pot and impregnation methods could be attributed to their different structures including textural structure and the dispersion of supported metal oxide species.

References

(1) Taylor, M. N.; Carley, A. F.; Davies, T. E.; Taylor, S. H. *Top. Catal.* **2009,** *52*, 1660. doi: 10.1007/s11244-009-9307-0

(2) Liu, Y. M.; Feng, W. L.; Li, T. C.; He, H. Y.; Dai, W. L.; Huang, W.; Cao, Y.; Fan, K. N. *J. Catal.* **2006,** *239*, 125. doi: 10.1016/j.jcat.2005.12.028

(3) Ying, F.; Li, J. H.; Huang, C. J.; Weng, W. Z.; Wan, H. L. *Catal. Lett.* **2007,** *115*, 137. doi: 10.1007/s10562-007-9079-8

(4) Abello, M. C.; Gomeza, M. F.; Ferretti, O. *Appl. Catal. A: Gen.* **2001,** *207*, 421. doi: 10.1016/S0926-860X(00)00680-3

(5) Chen, K.; Xie, S.; Bell, A. T.; Iglesia, E. *J. Catal.* **2001,** *198*, 232. doi: 10.1006/jcat.2000.3125

(6) Watson, R. B.; Ozkan, U. S. *J. Catal.* **2000,** *191*, 12. doi: 10.1006/jcat.1999.2781

(7) Li, J. H.; Wang, C. C.; Huang, C. J.; Sun, Y. F.; Weng, W. Z.; Wan, H. L. *Appl. Catal. A: Gen.* **2010,** *382*, 99. doi: 10.1016/j.apcata.2010.04.034

(8) Davies, T. E.; Garcia, T.; Solsona, B.; Taylor, S. H. *Chem. Commun.* **2006,** 3417.

(9) Zhao, D. Y.; Feng, J. L.; Huo, Q. S.; Melosh, N.; Fredrickson, G. H.; Chmelka, B. F.; Stucky, G. D. *Science* **1998,** *279*, 548. doi: 10.1126/science.279.5350.548

(10) Niesz, K.; Yang, P.; Somorjai, G. A. *Chem. Commun.* **2005,** 1986.

(11) Yuan, Q.; Yin, A. X.; Luo, C.; Sun, L. D.; Zhang, Y. W.; Duan, W. T.; Liu, H. C.; Yan, C. H. *J. Am. Chem. Soc.* **2008,** *130*, 3465. doi: 10.1021/ja0764308

(12) Stacy, M. M.; Pasquale, F. F.; Mietek, J. *J. Am. Chem. Soc.* **2008,** *130*, 15210. doi: 10.1021/ja806429q

(13) Shen, W. H.; Komatsubara, K.; Hagiyama, T.; Yoshida, A.; Naito, S. *Chem. Commun.* **2009,** 6490.

(14) Wang, H. Y.; Ruckenstein, E. *Catal. Lett.* **2001,** *75*, 13. doi: 10.1023/A:1016719703118

(15) Kobayashi, Y.; Horiguchi, J.; Kobayashi, S.; Yamazaki, Y.; Omata, K.; Nagao, D.; Konno, M.; Yamada, M. *Appl. Catal. A: Gen.* **2011,** *395*, 129. doi: 10.1016/j.apcata.2011.01.034

(16) Arnoldy, P.; Moulijin, J. A. *J. Catal.* **1985,** *93*, 38. doi: 10.1016/0021-9517(85)90149-6

(17) Jacobs, G.; Ji, Y.; Davis, B. H.; Cronauer, D.; Kropf, A. J.; Marshall, C. L. *Appl. Catal. A: Gen.* **2007,** *333*, 177. doi: 10.1016/j.apcata.2007.07.027

(18) Xiao, T. C.; Ji, S. F.; Wang, H. T.; Coleman, K. S.; Green, M. L. H. *J. Mol. Catal. A* **2001,** *175*, 111. doi: 10.1016/S1381-1169(01)00205-9

(19) Solsona, B.; Blasco, T.; Nieto, J. M. L.; Pena, M. L.; Rey, F.; Vidal-Moya, A. *J. Catal.* **2001,** *203*, 443. doi: 10.1006/jcat.2001.3326

(20) Zhang, X. J.; Liu, J. X.; Jing, Y.; Xie, Y. C. *Appl. Catal. A: Gen.* **2003,** *240*, 143. doi: 10.1016/S0926-860X(02)00426-X

(21) Cortes Corberan, V.; Jia, M. J.; EI-Haskouri, J.; Valenzuela, R. X.; Beltran-Porter, D.; Amoros, P. *Catal. Today* **2004,** *91–92*, 127.

(22) Karakoulia, S. A.; Triantafyllidis, K. S.; Lemonidou, A. A. *Microporous Mesoporous Mat.* **2008,** *110*, 157. doi: 10.1016/j.micromeso.2007.10.027

(23) Peña, M. L.; Dejoz, A.; Fornés, V.; Rey, E.; Vazquez, M. I.; Nieto, J. M. L. *Appl. Catal. A: Gen.* **2001,** *209*, 155.

(24) Buyevskaya, O. V.; Bruckner, A.; Kondratenko, E. V.; Wolf, D.; Baerns, M. *Catal. Today* **2001,** *67*, 369. doi: 10.1016/S0920-5861(01)00329-7

(25) Mitran, G.; Cacciaguerra, T.; Loridant, S.; Tichit, D.; Marcu, I. C. *Appl. Catal. A: Gen.* **2012,** *417–418*, 153.